Springer

Journal of Mechanical Science and Technology 23 (2009) 2169~2178

Journal of Mechanical Science and Technology

www.springerlink.com/content/1738-494x
DOI 10.1007/s12206-009-0435-z

Measurement of the normal acoustic impedance using beamforming method †

Jong Cheon Sun[1*], Chang Woo Shin[1], Hyung Jun Ju[1], Soon Kwon Paik[2] and Yeon June Kang[1]

[1]*Department of Mechanical and Aerospace Engineering, Seoul National University, Seoul, 151-744, Korea*
[2]*Hyundai & Kia Motors R&D Division, 772-1, Jangduk-Dong, Hwaseong-Si, Gyeonggi-Do, 445-706, Korea*

(Manuscript Received November 10, 2008; Revised February 6, 2009; Accepted February 27, 2009)

Abstract

A beamforming technique is introduced to measure the normal acoustic impedance at both normal and oblique incidence in a free field. In the proposed method, microphone array signals are decomposed into incident and reflected waves using an adaptive nulling algorithm, which is a type of beamforming algorithm. The acoustic impedance can then be calculated from the ratio of these two signals. To obtain better results, the pressure vector commonly used in array signal processing is replaced with the transfer function vector between each microphone, and the white Gaussian noise is suppressed by a wavelet shrinkage technique. For an accurate experimental setup, the incident and reflected angles are estimated by the multiple signal classification method with spatial smoothing. The experiments conducted in a semi-anechoic room show that the proposed method is efficient and accurate in measuring the normal acoustic impedance of sound-absorbing materials under a free field condition.

Keywords: Normal acoustic impedance; Adaptive nulling method; MUSIC method; Free-field

1. Introduction

One of the important problems in the area of sound field analysis of acoustic cavities (or enclosures) is how to measure the normal acoustic impedance of sound absorbing materials that are treated on their surfaces. To improve the accuracy of an interior sound prediction, it would be better to measure the normal acoustic impedance of an assembled component as it is, as its interior decorations or trims are often composed of layers of materials. Among the many methods to measure the normal acoustic impedance, the impedance tube method [1] is a well-known technique, as it gives reliable results over a wide frequency range. However, this method is limited when measuring the normal acoustic impedance of an assembled component. For this in a normal incidence case to be measured, uniform and circular samples are required.

Several methods for measuring normal acoustic impedance under a free field condition have been proposed to overcome the limitations of the shape and incidence angle. Allard et al. [2, 3] proposed a two - microphone method to measure normal acoustic impedance in a free field condition. In this method, the acoustic particle velocity is estimated by finite differentiation and the representative pressure value is estimated simply by taking the mean of the measured pressure signals. The normal acoustic impedance can then be calculated from these two values. Later, Tamura [4, 5] proposed a spatial Fourier transform method of measuring the reflection coefficient at oblique incidence. However, this method requires a large area of test material to take the spatial Fourier transform from many measurement points. Recently,

† This paper was recommended for publication in revised form by Associate Editor Hong Hee Yoo

*Corresponding author. Tel.: +82 2 880 7152, Fax.: +82 2 888 5950
E-mail address: sunje77@snu.ac.kr

Lanoye et al. [6] introduced a new method using a combined particle velocity – pressure sensor to measure the normal acoustic impedance. Although the method can provide very simple and fast measurements, it requires a sensor that is able to measure the particle velocity.

In this paper, a beamforming technique is applied to measure the normal acoustic impedance at both normal and oblique incidence in a free field. In the proposed method, pressures are measured using three microphones that are placed in a form of an array that is perpendicular to the surface of the test material. From the measured array signals, the incident and reflected waves are estimated by applying an adaptive nulling algorithm [7], and the reflection coefficient is calculated by the ratio of these two estimated waves. The normal acoustic impedance and absorption coefficient can then be calculated from the reflection coefficient. To obtain better results, the pressure vector commonly used in array signal processing is replaced by a transfer function vector composed of the transfer function between each microphone, and the white Gaussian noise is suppressed by using a wavelet shrinkage technique. Particularly, for an oblique incident case, incident and reflected angles are estimated by using the MUSIC method [9] for a precise experimental setup. The relative phase between each microphone is also calibrated b a tube method. Lastly, various experiments are conducted in a semi-anechoic chamber to verify the performance of the proposed method, and the results are compared with the values obtained by the impedance tube and theoretical method.

2. Beamforming method

Beamforming is a type of spatial filter that captures signals from a given direction using a microphone array. Thus, estimations of the incident and reflected signals or angles are possible by applying suitable beamforming algorithms, after which the reflection coefficients can be calculated from the ratio of the estimated signals. Particularly, as a number of beamforming algorithms may show degraded performance for mutually correlated waves, careful selection is required of the algorithms for a situation in which the incident wave is fully correlated with the reflected waves, as in this paper. The proposed method uses an adaptive nulling method to separate the incident and reflected waves, and it uses the MUSIC method to detect the angle of incidence from the microphone array signals. The performance of the adaptive nulling method is not related to the correlation of each signal as it uses not the signal cross-spectral matrix but a directional vector corresponding to each signal (Section 2.2). Although in the MUSIC method signal correlations are an important problem as in other beamforming algorithms, they can be mitigated by reducing the correlation with a spatial smoothing technique (Section 2.3).

The proposed method can be divided into two steps. The first involves the separation of incident and reflected waves from the measured array signals through the application of the adaptive nulling algorithm to calculate the normal acoustic impedance. The second involves an estimation of the incident and reflected angles using the MUSIC method for a precise experimental setup.

2.1 Geometry of the beamforming method and noise reduction

For the geometry shown in Fig. 1, a linear array of M microphones that receive incident and reflected signals from previously known directions θ and $\pi-\theta$ is considered under plane wave conditions. In the frequency domain, the measured pressure signals can be expressed in terms of the phase difference caused by the space between each microphone. This is written as

$$\begin{bmatrix} p_0(\omega) \\ p_1(\omega) \\ \cdot \\ p_{M-1}(\omega) \end{bmatrix} = \begin{bmatrix} 1 & 1 \\ e^{-jkd\cos\theta} & e^{jkd\cos\theta} \\ \cdot & \cdot \\ e^{-jk(M-1)d\cos\theta} & e^{jk(M-1)d\cos\theta} \end{bmatrix} \begin{bmatrix} s_i(\omega) \\ s_r(\omega) \end{bmatrix} + \begin{bmatrix} n_0(\omega) \\ n_1(\omega) \\ \cdot \\ n_{M-1}(\omega) \end{bmatrix}, \quad (1)$$

where $j=\sqrt{-1}$, d is the distance between each microphone and θ is the incident and the reflected angle, and $s_i(\omega)$, $s_r(\omega)$ denote the incident and reflected signals at the first microphone, respectively. Additionally, $p_m(\omega)$ and $n_m(\omega)$ are the pressure value and the white Gaussian noise at the (m+1)-th microphone, respectively. For convenience, Eq. (1) can be expressed by using the directional vectors between the input signals and measured array signals,

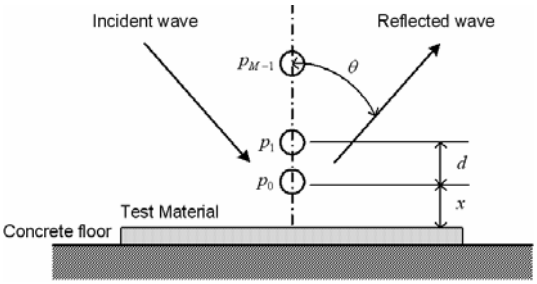

Fig. 1. Schematic illustration of the beamforming method.

as shown below.

$$\mathbf{p}(\omega) = [\mathbf{g}_i \ \mathbf{g}_r]\mathbf{s}(\omega) + \mathbf{n}(\omega) . \tag{2}$$

Here $\mathbf{p}(\omega)$ is the pressure vector, $\mathbf{s}(\omega)$ is input signal vector and $\mathbf{g}_i$, $\mathbf{g}_r$, column vectors of the matrix in right hand side of Eq. (1), are the directional vectors or beam vectors corresponding to the input signals $s_i(\omega)$ and $s_r(\omega)$, and $\mathbf{n}(\omega)$ is the noise vector. For simplicity, the frequency argument ω is omitted from this point.

If there is only one incident signal and if the reflected signals are caused by incident signal, the transfer functions between each microphone will have deterministic values because of the fully coherent sound field. Therefore, the pressure vector can be replaced by a modified pressure vector that consists of the transfer functions between the first and second pressure signals. That is,

$$\begin{bmatrix} H_0 \\ H_1 \\ . \\ H_{M-1} \end{bmatrix} = \begin{bmatrix} 1 & 1 \\ e^{-jkd\cos\theta} & e^{jkd\cos\theta} \\ . & . \\ e^{-jk(M-1)d\cos\theta} & e^{jk(M-1)d\cos\theta} \end{bmatrix} \begin{bmatrix} s_i' \\ s_r' \end{bmatrix} + \begin{bmatrix} n_0/p_0 \\ n_1/p_0 \\ . \\ n_{M-1}/p_0 \end{bmatrix} \tag{3}$$

or

$$\mathbf{p}' = [\mathbf{g}_i \ \mathbf{g}_r]\mathbf{s}' + \mathbf{n}/p_0 , \tag{4}$$

where H_m is the transfer function between the first and the (m+1)-th pressure signals as

$$H_m = \frac{p_m}{p_0} , \tag{5}$$

$\mathbf{p}'$ and $\mathbf{s}'$ are the modified pressure and signal vectors and s_i' and s_r' are s_i/p_0 and s_r/p_0, respectively. Here, the directional vectors in Eq. (3) and (4) are identical with those in Eqs. (1) and (2), although there is some change in the pressure and signal vectors.

Eqs. (3) and (4) may be more efficient than Eqs. (1) and (2) as they provide fast measurement and reduction of computational loads for practical measurement. For example, if Eqs. (1) and (2) are used to estimate the normal acoustic impedance, the computations must be repeated k times for k measurements. The normal acoustic impedance can be calculated by averaging the k obtained values. However, the use of Eqs. (3) and (4) will require only one computation, as each transfer function which is the element of those equations can be averaged by itself.

Considering that all measurements are conducted under a free field condition, the signal-to-noise ratio of the measured transfer functions may be relatively poor compared to that in the impedance tube. For an enhancement of the obtained values, reducing the white Gaussian noise is often an important issue. In this paper, a wavelet shrinkage technique was adapted to reduce the white Gaussian noise of the transfer functions. The wavelet which used in this paper was the Symlet wavelet, and its decomposition level was five. An overview of the wavelet shrinkage process is omitted here, as the applications of these techniques for de-noising have been widely verified in many papers [10-12]. However, in Section 3, it is possible to confirm that there was a meaningful difference between results with and without wavelet shrinkage in the experiments. For convenience, the noise term is omitted through the following deployment in this and the next sections; however, it is considered again in Section 2.3.

2.2 Calculation of the normal acoustic impedance

To estimate the incident signal s_i and the reflected signal s_r, an adaptive nulling method is utilized from the various beamforming algorithms. This is an algorithm that estimates the sought-after values by maximizing the signals from the incident or reflected angles while other directions are maintained at zero. The adaptive nulling algorithm finds the beam steering vector $\mathbf{q}_i$ that satisfies the next two conditions for an estimation of the incident signal [7].

$$\text{Maximize } |\mathbf{q}_i \cdot \mathbf{g}_i|, \tag{6}$$

$$\text{subject to } \|\mathbf{q}_i\| = 1, \tag{7}$$

$$\mathbf{q}_i \cdot \mathbf{g}_r = 0 . \tag{8}$$

Here, $\mathbf{q}_i$ is the beam steering vector that determines

the incident signal. This beam steering vector $\mathbf{q}_i$ can be easily found by using the orthogonal property of the vectors. Assuming that the beam steering vector is expressed as a linear combination of eigenvectors corresponding to the 2nd to the *M*-th eigenvalues of the matrix $\mathbf{g}_r\mathbf{g}_r^{\mathrm{H}}$, the following equation holds:

$$\mathbf{q}_i = \sum_{k=2}^{M} a_k \mathbf{e}_k \,, \tag{9}$$

where $\mathbf{e}_k$ is the *k*-th eigenvector of $\mathbf{g}_r\mathbf{g}_r^{\mathrm{H}}$ and a_k is unknown complex constant. As $\mathbf{g}_r\mathbf{g}_r^{\mathrm{H}}$ is a matrix with only one eigenvalue, $\mathbf{g}_r$ is clearly orthogonal to the beam steering vector $\mathbf{q}_i$ defined by Eq. (9). Therefore, the second condition of Eq. (8) can be fulfilled by this orthogonal property. To find the complex constant a_k that satisfies Eq. (6), the inner product is utilized with $\mathbf{q}_i$ and $\mathbf{g}_i$,

$$\mathbf{q}_i \cdot \mathbf{g}_i = \sum_{k=2}^{M} \left(a_k \mathbf{e}_k \cdot \mathbf{g}_i\right) = \mathbf{a} \cdot \mathbf{b} \,. \tag{10}$$

Here, $\mathbf{a}$ is a vector, the element of which is a_k, and $\mathbf{b}$ is also a vector consisting of the element $\mathbf{e}_k \cdot \mathbf{g}_i$. It is clear that the inner product of Eq. (10) has a maximum value when vector $\mathbf{a}$ is parallel to vector $\mathbf{b}$. Therefore, if a_k is defined as the next equation, the first condition of Eq. (6) is also satisfied.

$$a_k = b_k = \mathbf{e}_k \cdot \mathbf{g}_i \,. \tag{11}$$

Finally, by applying the Eq. (7) with Eq. (9) and (11), the beam steering vector $\mathbf{q}_i$ can be determined by

$$\mathbf{q}_i = \frac{\sum_{k=2}^{M} \left(\mathbf{e}_k \cdot \mathbf{g}_i\right)\mathbf{e}_k}{\left\| \sum_{k=2}^{M} \left(\mathbf{e}_k \cdot \mathbf{g}_i\right)\mathbf{e}_k \right\|} \,. \tag{12}$$

The incident signal can be estimated by taking the inner product with the beam steering vector $\mathbf{q}_i$ and the modified pressure vector of Eq. (4).

$$\mathbf{q}_i \cdot \mathbf{p}' = \mathbf{q}_i \cdot [\mathbf{g}_i \ \mathbf{g}_r]\mathbf{s}' = (\mathbf{q}_i \cdot \mathbf{g}_i)\mathbf{s}' = c_i s_i' \,. \tag{13}$$

Here, c_i is the complex constant $\mathbf{q}_i \cdot \mathbf{g}_i$. Additionally, the reflected signal is eliminated by the beam steering vector $\mathbf{q}_i$, and the incident signal is amplified by the complex constant c_i in Eq. (13) in spite of the full correlation between each signal. The modified incident signal s_i' can then be estimated by the following procedure:

$$s_i' = s_i / p_0 = \left(\mathbf{q}_i \cdot \mathbf{p}'\right) / \left(\mathbf{q}_i \cdot \mathbf{g}_i\right) . \tag{14}$$

The modified reflected signal s_r' can be also estimated by a repetition of the procedures from Eq. (6) to Eq. (14).

$$s_r' = s_r / p_0 = \left(\mathbf{q}_r \cdot \mathbf{p}'\right) / \left(\mathbf{q}_r \cdot \mathbf{g}_r\right) . \tag{15}$$

Here, $\mathbf{q}_r$ is a beam steering vector that is calculated from the two conditions, Eqs. (6) and (8) replaced $\mathbf{g}_i$ with $\mathbf{g}_r$. From Eqs. (14) and (15), the reflection coefficient is calculated from the ratio of the modified incident and reflected signals.

$$R(\theta) = \frac{s_r}{s_i} \mathrm{e}^{-\mathrm{j}k2x\cos\theta} = \frac{s_r'}{s_i'} \mathrm{e}^{-\mathrm{j}k2x\cos\theta} \,, \tag{16}$$

where x is the distance from the surface of the material to the position of the first microphone. In Eq. (16), the phase term expressed as the exponential function is a factor that calibrates the phase difference caused by the measurement at the location apart from the surface of the test material.

Finally, the normal specific acoustic impedance and absorption coefficient are calculated from the obtained reflection coefficient,

$$z(\theta) = \frac{Z(\theta)}{\rho c} = \frac{1}{\cos\theta} \frac{1 + R(\theta)}{1 - R(\theta)} \,, \tag{17}$$

$$\alpha(\theta) = 1 - |R(\theta)|^2 \,, \tag{18}$$

where $Z(\theta)$ is the normal acoustic impedance and ρ and c are the air density and the speed of sound in air, respectively.

2.3 Estimation of the incident and reflected angle

In the process of measuring the normal acoustic impedance, the speaker must be located far from the test material to satisfy the plane wave condition. Therefore, it may be difficult to set the speaker with the precise angle of incidence. For a precise experimental setup, the MUSIC method was utilized to estimate the angles of incidence and reflection. As the performance of MUSIC may be seriously degraded by the signal correlation, a spatial smoothing technique was adapted in order to reduce the coherence. In this section, an overview of the MUSIC method with spatial smoothing is briefly presented. A more detailed account can be found in the literature (see refs. 8, 15, 16).

A cross spectral matrix of a modified pressure vector in Eq. (4) is considered such that

$$\mathbf{R}_{\mathbf{p}'\mathbf{p}'} = E[\mathbf{p}'\mathbf{p}'^{\mathrm{H}}] = [\mathbf{g}_i \ \mathbf{g}_r]\mathbf{R}_{\mathbf{s}'\mathbf{s}'}[\mathbf{g}_i \ \mathbf{g}_r]^{\mathrm{H}} + \sigma_n'^2 \mathbf{I} \,, \tag{19}$$

where notation E is the expectation operator, $\mathbf{R}_{\mathbf{s}'\mathbf{s}'}$ is the signal cross-spectral matrix $\mathrm{E}[\mathbf{s}'\mathbf{s}'^{\mathrm{H}}]$ and $\sigma_n'^2$ is

σ_n^2 / P_0^2 when $\sigma_n^2 = E[n_i n_i^{\mathrm{H}}]$ and $P_0^2 = \mathrm{E}[p_0 p_0^{\mathrm{H}}]$. Here, $\mathbf{R}_{s's'}$ must be singular as the incident signal is fully correlated with the reflected signals generated by it. In further processing, this singular condition will prevent eigenvalue grouping corresponding to signal-plus-noise and noise subspace segmentation. To succeed with the process of the MUSIC method, the coherence between two signals must be reduced by various signal processing techniques. In this paper, spatial smoothing was employed to do this.

Spatial smoothing reduces the coherence by averaging the cross-spectral matrices computed for several sub-arrays. As shown in Fig. 2, the array of four microphones is divided into overlapping sub-arrays of three microphones. The cross-spectral matrix $\mathbf{R}_{p'p'}$ can be recomputed by averaging the cross-spectral matrices of each sub-array.

$$\bar{\mathbf{R}}_{p'p'} = \frac{1}{4}\sum_{k=1}^{2}\left(\mathbf{R}_k^f + \mathbf{R}_k^b\right), \tag{20}$$

where $\bar{\mathbf{R}}_{p'p'}$ is the averaged cross spectral matrix (3 by 3) and $\mathbf{R}_k^f$ and $\mathbf{R}_k^b$ are the forward and conjugate backward cross spectral matrices computed from the *k*-th sub-array. The forward and conjugate backward cross spectral matrix can be calculated as

$$\mathbf{R}_k^f = E[\mathbf{f}_k \mathbf{f}_k^{\mathrm{H}}], \quad k = 1,2, \tag{21}$$

$$\mathbf{R}_k^b = (E[\mathbf{b}_k \mathbf{b}_k^{\mathrm{H}}])^*, \quad k = 1,2, \tag{22}$$

where $\mathbf{f}_k = [H_{k-1}\ H_k\ H_{k+1}]^T$ and $\mathbf{b}_k = [H_{k+1}\ H_k\ H_{k-1}]^T$, and the mark * denotes the conjugate operator. By replacing the cross-spectral matrix $\mathbf{R}_{p'p'}$ with $\bar{\mathbf{R}}_{p'p'}$ in Eq. (19), the singular condition caused by the coherence between the two signals can be removed while reducing the array size by three [8].

To estimate the angle of incidence, the eigenvalue decomposition of $\bar{\mathbf{R}}_{p'p'}$ is considered.

$$\bar{\mathbf{R}}_{p'p'} = \sum_{l=1}^{3} \lambda_q \mathbf{v}_q \mathbf{v}_q^{\mathrm{H}}, \tag{23}$$

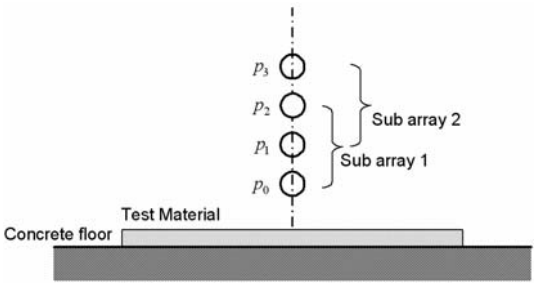

Fig. 2. Decomposition of the line array into two overlapping sub-arrays.

where λ_l is the *l*-th eigenvalue and $\mathbf{v}_l$ is the eigenvector corresponding to it. As the matrix $\bar{\mathbf{R}}_{p'p'}$ is composed of two signals with the level of coherence reduced by spatial smoothing, the first and second eigenvalues correspond to the signal-plus-noise subspace and the third eigenvalue is related to the noise subspace. Therefore, the third eigenvalue is

$$\lambda_3 = \sigma_n'^2. \tag{24}$$

From relationship between the eigenvalue and the eigenvector, the next equation can be deployed.

$$(\bar{\mathbf{R}}_{p'p'} - \sigma_n'^2 \mathbf{I})\mathbf{v}_3 = 0. \tag{25}$$

By substituting Eq. (19) into Eq. (25), following equation can be obtained as

$$[\mathbf{g}_i\ \mathbf{g}_r]\mathbf{R}_{s's'}[\mathbf{g}_i\ \mathbf{g}_r]^{\mathrm{H}}\mathbf{v}_3 = 0. \tag{26}$$

Eq. (26) implies that each beam steering vector $\mathbf{g}_i$ or $\mathbf{g}_r$ is orthogonal to the eigenvector associated with the noise subspace, as the signal correlation matrix $\mathbf{R}_{s's'}$ is non-singular and the beam steering matrix $[\mathbf{g}_i\ \mathbf{g}_r]$ has a full rank [13]. Thus, Eq. (26) can be written as

$$[\mathbf{g}_i\ \mathbf{g}_r]^{\mathrm{H}}\mathbf{v}_3 = 0. \tag{27}$$

Finally, the MUSIC power is given by

$$P_{MUSIC} = \frac{1}{\mathbf{g}_t^H \mathbf{v}_3}, \tag{28}$$

where $\mathbf{g}_t$ is the directional vector corresponding to direction θ_t. As the MUSIC power has peak values that result from the orthogonal property when the trial vector $\mathbf{g}_t$ is exactly parallel to the incident and the reflected beam steering vectors $\mathbf{g}_i$ and $\mathbf{g}_r$, the angles of incidence and reflection are estimated by determining the peak values of the MUSIC results. Given that the MUSIC algorithm is highly sensitive to the precision of the experimental setup, each microphone must be put on its precise point.

3. Measurement of the normal acoustic impedance and discussion

3.1 Relative phase calibration

In the proposed method, the measured normal acoustic impedance may be sensitive to the phase difference between each microphone as the directional vectors are dependent on the phase difference,

as shown in Eq. (1) or (3). Particularly, at low frequencies, although the absolute phase error of the transfer functions between each microphone is small, the relative phase error increases, as the wave length is much longer than the space between the microphones. To obtain meaningful data at lower frequencies, it is essential to calibrate the relative phase error between each microphone.

We employed the tube method to calibrate the phase error at low frequency, as shown in Fig. 3. Microphones used to measure the normal acoustic impedance were arranged at the end of the tube. To prevent the generation of a mode in the tube, the end of the tube was closed by using absorption material. At the other side, one speaker was set to radiate the pressure signal under the plane wave condition. If the measured transfer function from the first to the (m+1)-th microphone is H_m^{cal}, the calibrated transfer function can be calculated by the next equation,

$$H_m = H_m^{mea} \big/ H_m^{cal} , \tag{29}$$

where H_m^{mea} is the measured transfer function from the first to the (m+1)-th microphone in a free field.

3.2 Measurement of the normal acoustic impedance and discussion

Shown in Fig. 4 is the experimental setup for the measurements of the normal acoustic impedance at normal incidence in a semi-anechoic room. The test material of glass wool of 1 cm thickness was placed on the concrete floor. Its size was 1m by 1m. One speaker was set at a height of 2 m in a vertical direction relative to the floor in order to satisfy the plane wave condition. The array consisted of B&K Type 4935 microphones, and the distance from the surface of the test material to the first microphone was 0.4 cm. The space between each microphone was 0.7 cm. The data acquisition equipment and software were LMS SCADAS III and CADA-X, respectively. The transfer functions between each microphone were obtained by averaging 1500 trials when the FFT size and frequency resolution were 8192 and 8 Hz, respectively.

The effect of de-noising with the wavelet shrinkage technique was considered in the first experiment. The line array consisted of three microphones, and the transfer functions between the first and the additional microphones were measured and calibrated, as provided in section 3.1. Fig. 5 shows the average transfer function between the first and second microphones with and without de-noising by the Symlet wavelet and at a decomposition level of five. As shown in this figure, the transfer function with de-noising is slightly smoother than the original values. Additionally, it is readily apparent that the phase values at low frequencies below 1000 Hz were very close to zero, as mentioned in section 3.1. Next, from these two sets of transfer functions, reflection coefficients and absorption coefficients were calculated by using the adaptive

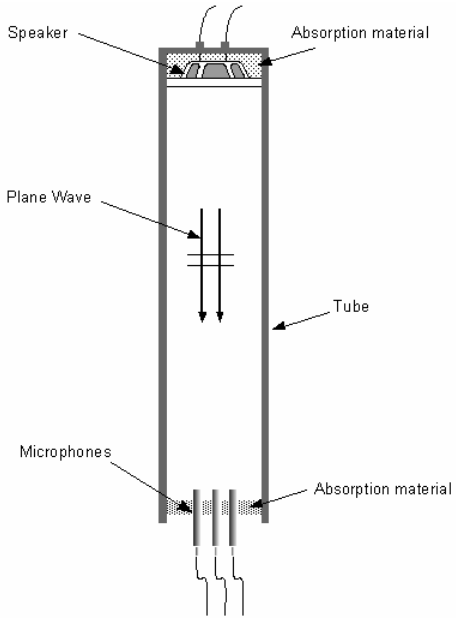

Fig. 3. Experimental setup of the relative phase calibration.

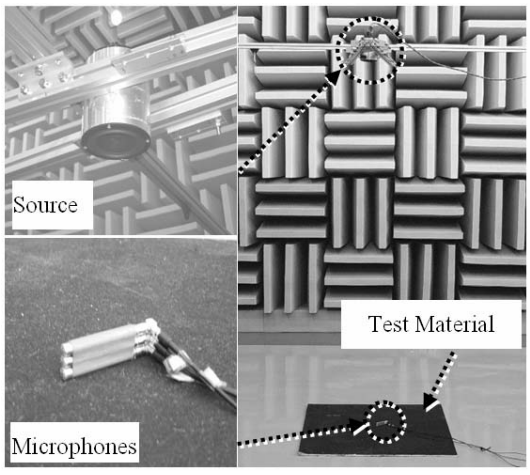

Fig. 4. Experimental setup of the measurement of the normal acoustic impedance at normal incidence.

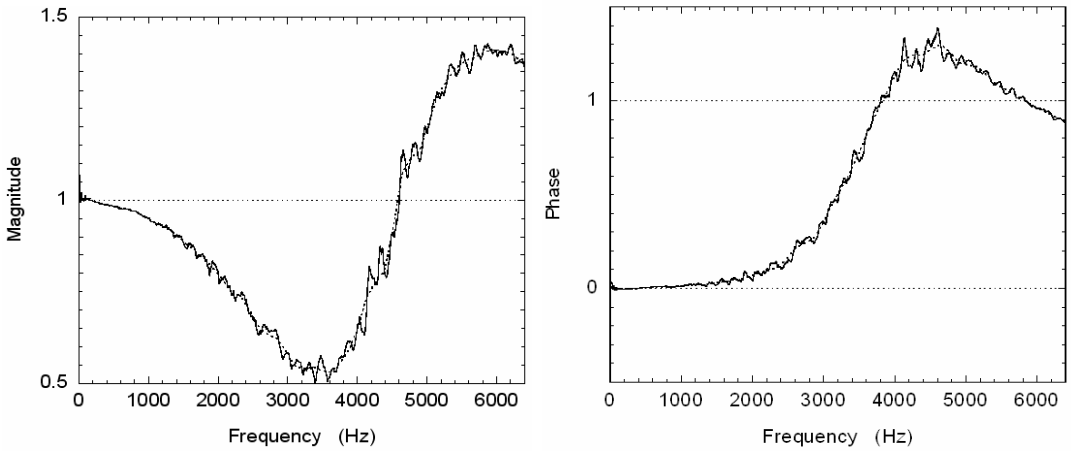

(a) (b)

Fig. 5. Comparison of the transfer function with and without de-noising. (a) and (b) are the magnitude and phase of the transfer function between the first and second microphones. ———, transfer function without de-noising; - - - - -, transfer function with de-noising.

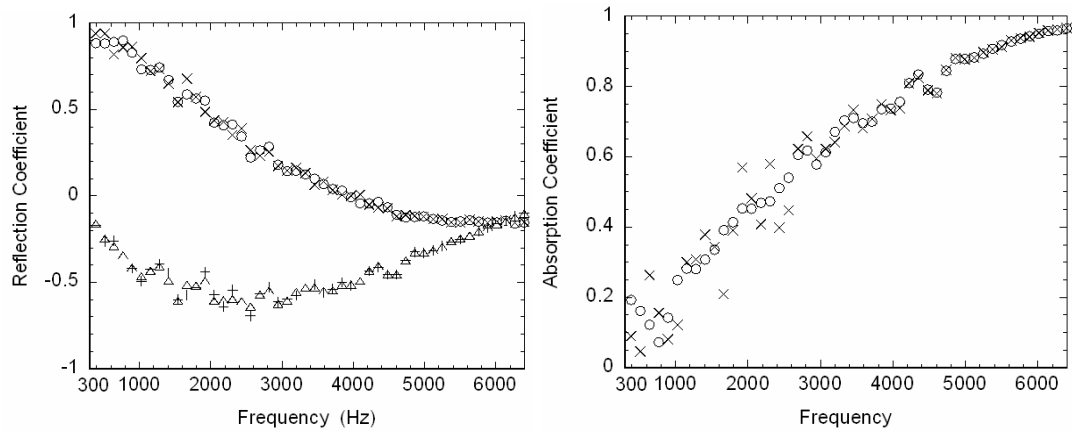

(a) (b)

Fig. 6. Comparison of the measured results by the beamforming method with and without de-noising. (a) Reflection coefficient, (b) Absorption coefficient. ○, △, results with de-noising; ×, +, results without de-noising.

nulling method. It is shown in Fig. 6 that the results with de-noising were less spread compared to those without de-noising. Particularly, the effect of de-noising was significant concerning the results of the absorption coefficients as shown in Fig. 6 (b). These results show that de-noising with wavelet shrinkage can be a good means of overcoming the noisy condition.

To verify the values obtained by the proposed method, the normal acoustic impedance and reflected coefficient were also measured with a B&K two-microphone impedance measurement tube (Type 4206). As shown in Fig. 7, the values obtained by the beamforming method with wavelet de-noising are in good agreement with the data from the impedance tube in the frequency range 400 to 6400 Hz.

At low frequencies below 400 Hz, the results by the proposed method are very different from those obtained using impedance tube method. One reason for this error is that the distance between each microphone was very short in comparison with the wavelengths of the low frequencies. However, the error cannot be reduced by increasing the space between each microphone, as the plane wave condition will not be satisfied when it is distant from the surface due to the finite sample size

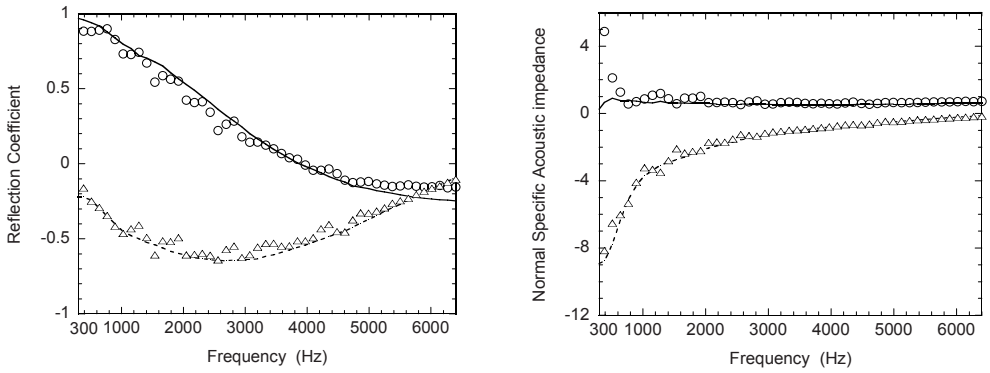

(a) (b)

Fig. 7. Comparison of the measured results with the impedance tube and the beamforming methods. (a) Reflection coefficient, (b) Normal acoustic impedance. ———, impedance tube method (real part); - - - - - - - -, impedance tube method (imaginary part); ○, beamforming method (real part); △, beamforming method (imaginary part).

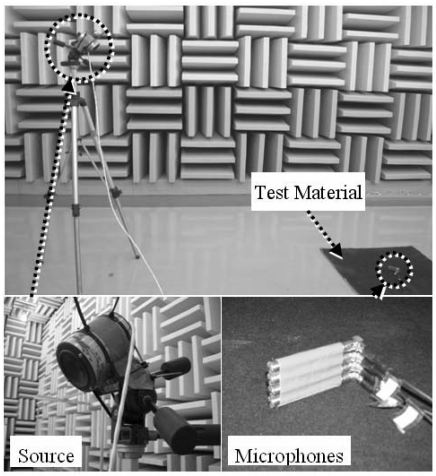

Fig. 8. Experimental setup of the measurement of the normal acoustic impedance at oblique incidence.

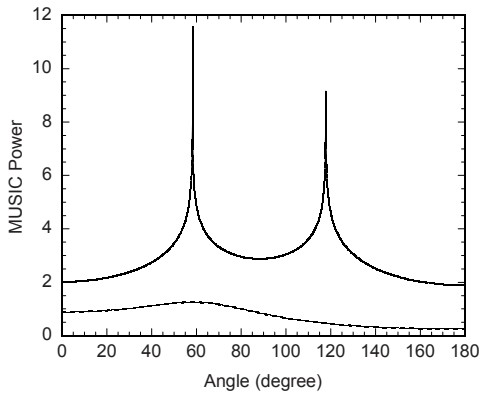

Fig. 9. Comparison of the MUSIC powers with and without spatial smoothing at 6000 Hz. By determining the peak value at the left side in this figure, an incident angle of approximately 58° could be estimated. ———, MUSIC power with spatial smoothing; - - - - - - - -, MUSIC power without spatial smoothing.

The normal acoustic impedance was then measured for the oblique incidence case. Before computing the normal acoustic impedance, the incident and reflected angles were estimated by the MUSIC algorithm. As shown in Fig. 2 and Fig. 8, four microphones (B&K Type 4935) were set on a vertical line against the surface of the test material. The distance between each microphone was 0.7 cm. One speaker was located 2 m from the array. These experiments were conducted at a very high frequency of 6000 Hz, as the space between each microphone was very close and because the resolution of the MUSIC results is generally fine at higher frequencies, although the incident and reflected angles are independent of the frequency. Fig. 9 shows the results of the MUSIC method with and without spatial smoothing.

As shown in these results, the incident angle could be clearly estimated using MUSIC with spatial smoothing, whereas the result without spatial smoothing failed to detect the angles. The normal acoustic impedance for the incident angle estimated by MUSIC was calculated by beamforming method with wavelet de-noising. Although four microphones were set to measure the pressure signal, three microphones located close to the surface of the test material were used to calculate the normal acoustic impedance. To verify the results measured by the beamforming method, theoretical values were obtained by the transfer matrix method [14] using the properties in Table 1.

Table 1. Properties of the test material.

Thickness (mm)	10
Bulk Modulus (kg/m^3)	81.81
Flow resistivity (MKS Rayls / m)	48210
Structure Factor (-)	1.05
Porosity (-)	0.88
Viscous characteristic length (μm)	46.46
Thermal characteristic length (μm)	128.50

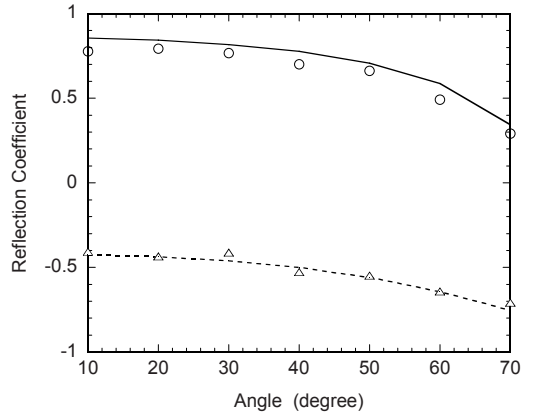

(a)

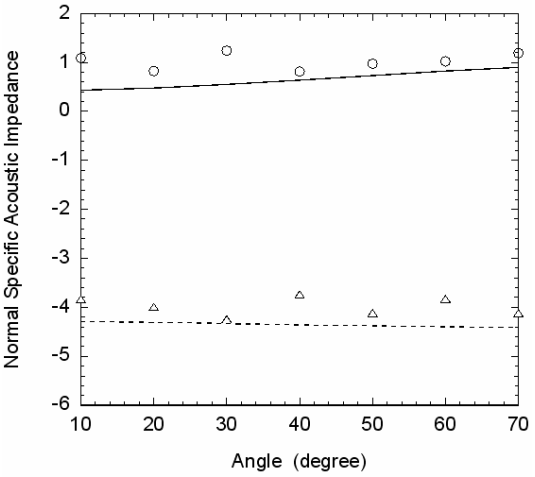

(b)

Fig. 10. Comparison of the measured results with theoretical and beamforming methods for the oblique incidence at 1000 Hz. (a) Reflection coefficient, (b) Normal acoustic impedance. ———, theoretical values (real part); - - - - - - - -, theoretical values (imaginary part); ○, beamforming method (real part); △, beamforming method (imaginary part).

These properties, with the exception of the thickness, were also estimated by a numerical method and normal absorption coefficient [13]. Figure 10 shows a comparison of the theoretical values and experimental results at 1000 Hz. In these figures, the results obtained by the proposed method are in good agreement with the theoretical values.

4. Conclusion

The normal acoustic impedances at normal and oblique incidence were measured by a new beamforming method in a free field. The accuracy of the measured normal acoustic impedance could be improved by using a transfer function vector which had the white Gaussian noise reduced by the wavelet shrinkage. A speaker and microphone array were located at precise directions or positions by estimating the incident and reflected angles from MUSIC with spatial smoothing. The proposed method was verified through comparisons with the impedance tube data and theoretical values. Particularly, for the normal incidence case, the values obtained by the proposed method were in good agreement with the values obtained using the impedance tube in a range of 400 to 6400 Hz.

References

[1] ASTM E1050 Standard test method for impedance and absorption of acoustical materials using a tube, two microphones and a digital frequency analysis system, *ASTM,* E1050-EBGL (1998).

[2] J. F. Allard and B. Sieben, Measurements of acoustic impedance in a free field with two microphones and a spectrum analyzer, *J. Acoust. Soc. Am*. 77 (4) (1985) 1617-1618.

[3] Y. Champoux, J. Nicolas and J. F. Allard, Measurement of acoustic impedance in a free field at low frequencies, *Journal of Sound and Vibration*, 125 (2) (1988) 313-323.

[4] M. Tamura, Spatial Fourier transform method of measuring reflection coefficients at oblique incidence. I: Theory and numerical examples, *J. Acoust. Soc. Am.* 88 (5) (1985) 2259-2264.

[5] M. Tamura, J. F. Allard and D. Lafarge, Spatial Fourier-transform method for measuring reflection coefficients at oblique incidence. II: Experimental results, *J. Acoust. Soc. Am.* 97(4) (1995) 2255-2262.

[6] R. Lanoye, G.. Vemeir, and W. Lauriks, Measuring

the free field acoustic impedance and absorption coefficient of sound absorbing materials with a combined particle velocity-pressure sensor, *J. Acoust. Soc. Am.* 119 (5) (2006) 2826-2831.

[7] Y. J. Kang and E. S. Hwang, Beamforming-based Partial Field Decomposition in NAH, *Journal of Sound and Vibration*, 314 (2008) 867-884.

[8] T. -J. Shan, M. Wax and T. Kailath, On spatial smoothing for direction-of-arrival estimation of coherent signals, *IEEE Transactions on Acoustics, Speech and Signal Processing*, ASSP-33 No. 4 (1985) 806-811.

[9] M. R. Bai and J. Lee, Industrial noise source identification by using an acoustic beamforming, *system Transactions of ASME*, 120 (1998) 426-433.

[10] Y. -Y. Shih, J. -C. Chen and R. -S. Liu, Development of wavelet de-noising technique for PET images, *Computerized Medical Imaging and Graphics*, 29 (2005) 297-304.

[11] Y. Y. Kim and J.-C., Hong Frequency response function estimation via a robust wavelet de-noising method, *Journal of Sound and Vibration*, 244(4) (2001) 635-649.

[12] A. Bakhtazad, A. Palazoglu and J. Romagnoli, Process trend analysis using wavelet-based de-noising, *Control Engineering Practice* 8 (2000) 657-663.

[13] Y. J. Kim, Y. J. Kang and J. S. Kim, Parameters estimation and performance prediction of acoustical materials, *ICSV 12 Proceedings* (2005).

[14] Y. J. Kang, *Studies of Sound Absorption by and Transmission through Layers of Elastic Noise Control Foams: Finite Element Modeling and Effects of Anisotropy*, Ph.D. dissertation, School of Mechanical Engineering, Purdue University (1994).

[15] J. C. Liberti Jr. and T. S. Rappaport, *Smart antennas for wireless communications: IS-95 and Third Generation CDMA Applications*, Prentice Hall, Upper Saddle River, (1999) 257-260.

[16] D. H. Johnson and D. E. Dudgeon, *Array signal processing: concepts and techniques*, Prentice-Hall, Englewood Cliffs, NJ (1993).

Jongcheon Sun received his B.S. degree in Mechanical Engineering from Korea University, Korea, in 2002. He is currently in the Unified Master's and Doctor's course at the School of Mechanical and Aerospace Engineering at Seoul National University, Korea. His research areas are acoustic holography and beamforming.